myo-Inositol oxygenase: molecular cloning and expression of a unique enzyme that oxidizes *myo*-inositol and D-*chiro*-inositol

Ryan J. ARNER, K. Sandeep PRABHU, Jerry T. THOMPSON, George R. HILDENBRANDT, Andrew D. LIKEN and C. Channa REDDY[1]

Department of Veterinary Science and Center for Molecular Toxicology and Carcinogenesis, 115 Henning Building, The Pennsylvania State University, University Park, PA 16802, U.S.A.

myo-Inositol oxygenase (MIOX) catalyses the first committed step in the only pathway of *myo*-inositol catabolism, which occurs predominantly in the kidney. The enzyme is a non-haem-iron enzyme that catalyses the ring cleavage of *myo*-inositol with the incorporation of a single atom of oxygen. A full-length cDNA was isolated from a pig kidney library with an open reading frame of 849 bp and a corresponding protein subunit molecular mass of 32.7 kDa. The cDNA was expressed in a bacterial pET expression system and an active recombinant MIOX was purified from bacterial lysates to electrophoretic homogeneity. The purified enzyme displayed the same catalytic properties as the native enzyme with K_m and k_{cat} values of 5.9 mM and 11 min^{-1} respectively. The pI was estimated to be 4.5. Preincubation with 1 mM Fe^{2+} and 2 mM cysteine was essential for the enzyme's activity. D-*chiro*-Inositol, a *myo*-inositol isomer, is a substrate for the recombinant MIOX with an estimated K_m of 33.5 mM. Both *myo*-inositol and D-*chiro*-inositol have been implicated in the pathogenesis of diabetes. Thus an understanding of the regulation of MIOX expression clearly represents a potential window on the aetiology of diabetes as well as on the control of various intracellular phosphoinositides and key signalling pathways.

Key words: diabetes, D-glucuronate, kidney, mono-oxygenase, pig.

INTRODUCTION

myo-Inositol and its various biochemical derivatives are widely distributed in mammalian tissues, higher plants, fungi and some bacteria, where they are important in many aspects of cellular regulation including membrane structure, signal transduction and osmoregulation [1–3]. The first committed step in the metabolism of *myo*-inositol occurs predominantly in the kidney and involves the oxidative cleavage of the ring to give D-glucuronic acid, as shown in Figure 1 [4,5]. The D-glucuronate formed in animals by this mechanism is successively converted in subsequent steps to L-gulonate, 3-oxo-L-gulonate, L-xylulose, xylitol, D-xylulose and D-xylulose-5-phosphate, which then enters the pentose phosphate cycle [6].

myo-Inositol oxygenase (MIOX, EC 1.13.99.1) is of considerable interest physiologically because it catalyses the first committed step in the only pathway of *myo*-inositol catabolism. This reaction is therefore an important determinant of inositol levels *in vivo*. The enzyme was first reported in 1957 in rat kidney extracts [5] and was subsequently purified from rat kidney [7,8] and oat seedlings [9]. Because MIOX isolated from those sources was found to be very unstable, little information on its mechanism was determined and few detailed characteristics of the protein were ascertained. In the early 1980s we purified MIOX to electrophoretic homogeneity from pig kidney [10]. Of particular importance in developing the purification procedure was the finding that although the enzyme becomes catalytically less active during purification, it could be stabilized more easily by reconstitution with cysteine and ferrous iron [10]. This enabled us to study some of the basic physical and catalytic properties of the purified enzyme [11] as well as some of the preliminary mechanistic studies [12,13]. MIOX is an enzyme containing non-haem iron and catalyses a four-electron oxidation with the transfer of only one atom of oxygen into the product.

The catalytic mechanism of MIOX is unique among non-haem iron internal mono-oxygenases in biological systems and there are very few enzymes that catalyse an oxidative glycol cleavage reaction as MIOX does. Nevertheless, the purification of the enzyme from kidneys to electrophoretic homogeneity in adequate amounts for detailed mechanistic studies eluded and frustrated many investigators. Consequently, very little progress has been made on this enzyme in the intervening 20 years.

Any examination of physiological roles for *myo*-inositol and MIOX, the prime enzyme in its catabolism, requires a consideration of the possible impact of MIOX-modulated *myo*-inositol concentrations on signal transduction pathways, which involve inositol phosphates. As seen in the review by Majerus [2], the metabolism of inositol phosphates is quite complex and in mammalian systems is channelled through phosphatidylinositol as the common precursor of the important signalling molecules Ins(1,4,5)P_3 and Ins(1,4)P_2 as well as diacylglycerol. The production of intracellular *myo*-inositol-derived second messengers seems to be specifically involved in the control of cellular events such as the spatial and temporal organization of key signalling pathways, the rearrangement of the actin cytoskeleton and intracellular vesicle trafficking [14]. Although little linkage has been drawn between *myo*-inositol concentrations and phosphoinositide metabolism, there is some evidence of altered signal transduction and inositol phosphate metabolism in rat sciatic nerves during streptozotocin-induced diabetes [15]. Because levels of *myo*-inositol in diabetic animals are lower in the central nervous system, whereas the renal clearance of *myo*-inositol is

Abbreviations used: HIC, hydrophobic interaction chromatography; IPTG, isopropyl β-D-thiogalactoside; LB, Luria–Bertani; MIOX, *myo*-inositol oxygenase; RACE, rapid amplification of cDNA ends; rMIOX, recombinant MIOX.

[1] To whom correspondence should be addressed (e-mail ccr1@psu.edu).

The nucleotide sequence data reported will appear in DDBJ, EMBL and GenBank® Nucleotide Sequence Databases under the accession number AF401311.

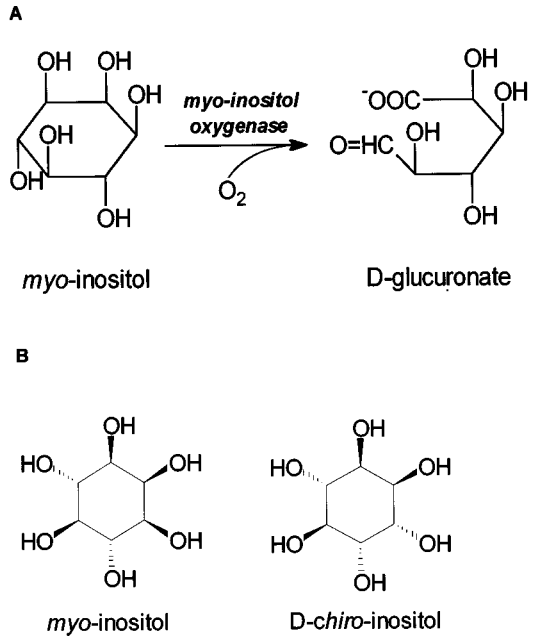

Figure 1 First step in the catabolism of *myo*-inositol (A) and the structures of *myo*-inositol and D-*chiro*-inositol (B)

enhanced, kidney MIOX levels might have a role in altered signal transduction. It is unclear how streptozotocin induces this effect and whether it precisely mimics diabetic neuropathy. However, it raises the prospect that modified *myo*-inositol levels might be important in understanding diabetic pathologies at the level of phosphoinositide signalling.

Although inositol catabolism in disease states such as diabetes has received little study, a large volume of work has been produced about altered levels of inositol in the diabetic state [16,17]. Of the physiological isomers of inositol, *myo*-inositol and D-*chiro*-inositol are associated with diabetic pathologies [17,18]. Intracellular depletion of *myo*-inositol is associated with complications including diabetic nephropathy [19–21], retinopathy [22], neuropathy [23,24] and diabetic cataract [25,26]. Most importantly, the presence of MIOX in the mammalian lens has been demonstrated for the first time [25]. It is the first direct evidence that MIOX might have a role in the secondary pathologies of diabetes, and given the apparent similarity between the factors involved in neuropathy, nephropathy and retinopathy [27–29] it is conceivable that MIOX might well be involved in all three pathologies. D-*chiro*-Inositol has been shown to be a component of an inositol phosphoglycan that mediates the action of insulin [30]. Infusion of the inositol phosphoglycan containing D-*chiro*-inositol in streptozotocin diabetic rats corrected the hyperglycaemic state [31,32]. The discovery of a common transporter protein with specificity for both *myo*-inositol and D-*chiro*-inositol, which is inhibited by glucose, supports the increased clearance of both inositol isomers during hyperglycaemia [33].

Thus *myo*-inositol and D-*chiro*-inositol seem to have a major role in the pathogenesis of diabetes and its related complications of nephropathy, retinopathy, neuropathy and cataract. An understanding of the major mechanism for the control of inositol metabolism at the level of MIOX might therefore open new windows to diabetic therapy. Here we report the cloning and expression of MIOX, which also exhibits significant enzyme activity towards D-*chiro*-inositol. Overexpression of this enzyme would allow us to undertake a more detailed understanding of the structure and function of this important protein.

EXPERIMENTAL

Pig kidney MIOX purification

The pig kidney MIOX purification protocol was as reported previously from our laboratory [10] with the following modifications. Immediately after animals were killed in local slaughterhouses, kidneys were collected and placed on ice. The tissue was minced, washed with ice-cold water and homogenized in a Waring blender in 25 mM sodium acetate buffer, pH 6.0, containing 1 mM GSH and 1 mM PMSF. All subsequent purification steps were performed with the 25 mM sodium acetate buffer, pH 6.0 (standard buffer). Crude homogenate was fractionated with $(NH_4)_2SO_4$ and the pellet from the 35–60 %-satd $(NH_4)_2SO_4$ fraction was collected, resuspended and dialysed against the standard buffer for further purification. This fraction was then subjected to anion-exchange chromatography on a DE-52 column; active fractions were pooled and concentrated. The MIOX activity pool was then applied to a Sephacryl-200 column for size-exclusion chromatography. Active fractions were collected, pooled, concentrated and subjected to chromatography on a phenyl-(hydrophobic interaction chromatography) (HIC) HPLC column.

Partial protein sequencing

The HIC-purified MIOX was separated by SDS/PAGE; 35 μg was blotted on a 0.2 μm PVDF membrane (Bio-Rad Laboratories, Hercules, CA, U.S.A.) in accordance with the manufacturer's instructions. The major 33 kDa band, which was determined as MIOX by several criteria, was excised from the membrane and submitted for amino acid sequencing to the Columbia University Protein Chemistry Core Facility (New York, NY, U.S.A.). The N-terminus was blocked, so two internal amino acid sequences were recovered. The purified protein was also used to prepare monoclonal antibodies in mice at The Pennsylvania State University Life Sciences Consortium Hybridoma Facility (University Park, PA, U.S.A.).

cDNA library construction

A pig kidney cDNA library was constructed with a SMART cDNA library construction kit from Clontech Laboratories (Palo Alto, CA, U.S.A.) in accordance with the manufacturer's instructions. In brief, mRNA from pig kidney was reverse transcribed with a poly(dT) primer and anchor primer. The single-stranded cDNA was amplified by PCR, digested and inserted into a λTriplEx2 vector. The vector was packaged with Gigapack Gold packaging extract (Stratagene, La Jolla, CA, U.S.A.) and the library was amplified in accordance with the manufacturer's indications.

PCR cloning of MIOX

Internal primer sequences were generated on the basis of known peptide sequences for PCR cloning from the pig kidney cDNA library. The sense primer (5′-CAGACAGTGGACTTCGTCAGGA-3′) and anti-sense primer (5′-GTGCCAGGGGTAGAAGGAGTGGAAC-3′) generated a product 531 bp in length. This amplimer was gel-purified and cloned into pGEM-T Easy vector (Promega, Madison, WI, U.S.A.) and sequenced at the

Penn State Nucleic Acid Facility (University Park, PA, U.S.A.) to compare the translated sequence with the peptide sequence obtained from tissue-purified MIOX. The remaining cDNA sequence was amplified by 5′ and 3′ rapid amplification of cDNA ends (RACE). 5′ RACE was performed with the internal anti-sense primer above and a sense primer (5′-GAAGCGCGCC-ATTGTGTTGGT-3′) based on the λTriplEx2 vector sequence. The 3′ RACE was performed with the sense internal primer above and CDSIII primer (Clontech). All PCR amplifications were performed with proofreading *Pfx* polymerase enzyme (Gibco BRL, Rockville, MD, U.S.A.) and amplimers were confirmed by sequencing both DNA strands at least in duplicate.

Expression of recombinant MIOX (rMIOX)

For bacterial expression of MIOX cDNA, an insert was constructed by PCR with pig kidney cDNA library as template. The full-length coding region was amplified with an *Nde*I site included in the sense primer (5′-GGAATTCCATATGAAGGACC-CAGACCCTTC-3′) and a *Bam*HI site in the anti-sense primer (5′-CGGGATCCCGTCACCAGCACAGGACA-3′). This PCR product was purified from a low-melting-point agarose gel, digested with *Nde*I and *Bam*I and then ligated into pET17b vector (Novagen, Madison, WI, U.S.A.), also digested with *Nde*I and *Bam*HI. The pET17b construct was transformed into DH5α competent *Escherichia coli* cells and screened by PCR for the presence of full-length MIOX cDNA and the proper orientation. Positive clones were grown and plasmid DNA was purified by plasmid miniprep kit (Promega). The plasmid was sequenced in triplicate to ensure the proper reading frame and polymerase fidelity. For expression, the pET17b/MIOX construct was transformed into BL21(DE3) cells (Novagen) and again screened by PCR for the presence of pET17b/MIOX. A positive colony was grown in Luria–Bertani (LB)/ampicillin medium as a starter culture for 5 h. Starter culture (2 ml) was then inoculated into 2 litres of LB/ampicillin medium supplemented with 20 mM *myo*-inositol and grown at 37 °C until D_{600} reached 0.6. The culture was induced with 1 mM isopropyl β-D-thiogalactoside (IPTG) for 4 h. The cells were pelleted by centrifugation at 10000 ***g*** and the pellet was frozen at −80 °C until the purification of rMIOX.

Purification of rMIOX

The frozen bacterial pellet was thawed on ice. All subsequent steps were performed at 4 °C unless otherwise mentioned. The pellet was ground in a mortar with glass beads (450–600 μm diameter; Sigma Chemical Co., St Louis, MO, U.S.A.) in 3 ml of standard buffer plus bacterial protease inhibitor cocktail. The lysate was transferred to a tube and the mortar was washed twice with an additional 3 ml of standard buffer; washings were pooled. The pooled lysate was sonicated briefly. Cell debris was pelleted by centrifugation at 20000 ***g*** for 15 min. $(NH_4)_2SO_4$ was added to the supernatant to 35 % saturation and stirred for 1 h. After centrifugation at 20000 ***g***, the concentration of $(NH_4)_2SO_4$ in the supernatant was brought to 60 % saturation and centrifuged again. The pellet from this fraction was recovered and dissolved in 1 ml of standard buffer, then dialysed overnight against 1000 vol. of standard buffer. The dialysed pellet was loaded on a DE-52 column (20 ml bed volume; 1.5 cm × 20 cm column) that had been pre-equilibrated overnight with standard buffer. The column was washed with 40 ml of buffer until A_{280} was less than 0.01. A linear gradient of 0–0.2 M KCl (100 ml of each) in standard buffer was used to elute DE-52-bound MIOX. Fractions were assayed for MIOX activity with an orcinol-based assay described previously [10] and were also analysed by SDS/PAGE. Active fractions were pooled and concentrated to approx. 1 ml volume and loaded on a Sephacryl 200 gel-filtration column (212 ml bed volume; 1.5 cm × 120 cm column). Fractions of 2.3 ml were collected, then assayed for MIOX activity and analysed by SDS/PAGE. Fractions with MIOX activity were pooled and concentrated.

Western immunoblot analysis

The purified rMIOX was subjected to SDS/PAGE [12.5 % (w/v) gel] and transferred to a nitrocellulose membrane (pore size 0.2 μm). The membrane was immersed in a blocking solution of TBS-T buffer [0.05 % Tween 20/0.1 M Tris/HCl/0.15 M NaCl (pH 7.5)] containing 5 % (w/v) BSA. This was followed by successive incubations overnight at 4 °C with hybridoma cell supernatant and at 37 °C for 60 min with anti-mouse IgM conjugated with horseradish peroxidase (dilution 1:2500). The blot was washed three times in TBS-T and developed by the enhanced chemiluminescence detection method (Pierce Chemical Co., Rockford, IL, U.S.A.).

MIOX assay

Enzyme activities were determined by an orcinol assay system as described previously [10]. Kinetic parameters for *myo*-inositol and D-*chiro*-inositol were determined by the same assay method. Activity measurements were taken for *myo*-inositol over a concentration range of 0.5–50 mM, and for D-*chiro*-inositol from 5–300 mM. K_m and k_{cat} values were calculated by regression analysis from Lineweaver–Burk plots.

Characterization of rMIOX

The molecular mass of the recombinant protein was investigated first. In addition to SDS/PAGE, a sample was submitted for electrospray MS determination at the Penn State Intercollegiate Mass Spectrometry Center (University Park, PA, U.S.A.). Also, the rMIOX was subjected to gel-filtration chromatography on a Sephacryl 200 column as described above. The purified rMIOX thus obtained was used for sedimentation equilibrium studies on a Beckman XL-1 analytical ultracentrifuge. Experiments were performed with 125 μl samples of the rMIOX at 0.2, 0.4 and 1.0 mg/ml concentrations in standard buffer. Scans of absorption against radius over a radial distance increment of 0.001 cm were collected at 12500 rev./min for 5 h, 15000 rev./min for 11 h, 17000 rev./min for 17 h and 50000 rev./min (Beckman An60Ti) for 19 h at 4 °C. The scanning absorption detection system was adjusted to measure solution absorbance at 250 and 280 nm against appropriate blanks. These results were collected at regular intervals until successive scans gave identical profiles, indicative of equilibrium. The experiment was repeated at all three protein concentrations in the presence of (1) *myo*-inositol (60 mM), (2) ferrous iron (Fe^{2+}) (1 mM) and cysteine (2 mM) and (3) *myo*-inositol plus Fe^{2+}/cysteine. The partial specific volume (v_B) was considered to be 0.73. Data were analysed to determine the molecular mass with the program ORIGIN (Microcal Software, Northampton, MA, U.S.A.). The rMIOX was loaded on a Reactive Blue 4 agarose column (bed volume 4 ml) to determine whether pig rMIOX displayed an affinity for NADPH. The column was washed with standard buffer and was eluted with 1 mM NADPH. The flow-through fraction and NADPH eluate were analysed by SDS/PAGE.

RESULTS

Purification of MIOX from pig kidneys

To obtain internal protein sequences on which to base PCR primer sequences for cloning, we purified pig kidney MIOX as described previously [10]. The yield of pure MIOX from 400 g of fresh tissue was 5.5 mg. HIC, which is a modification of the previously published procedure [10], was employed to purify MIOX, which was then used for amino acid sequencing (boxed area in Figure 2A). The purified MIOX consistently displayed one predominant band with a molecular mass of approx. 33 kDa (Figure 2B) and had a specific activity of 1250 nmol/min per mg

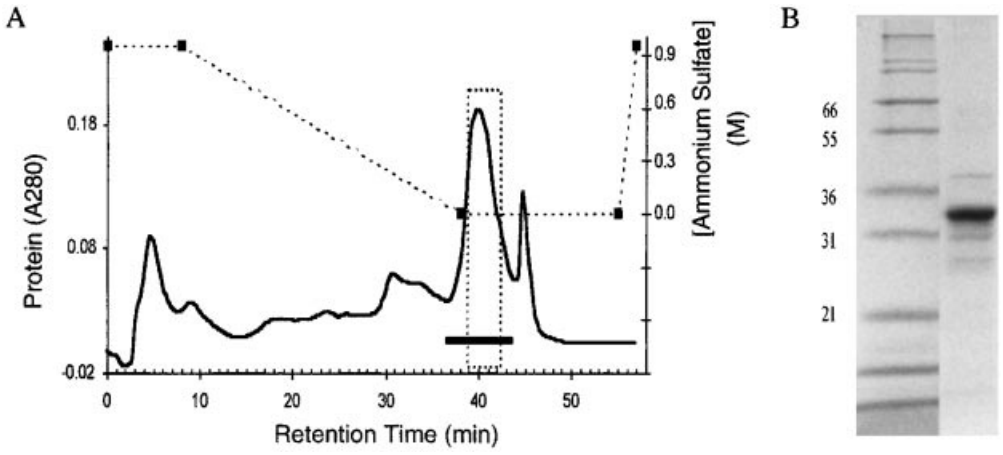

Figure 2 Purification of native MIOX

(**A**) Phenyl-HIC purification of the gel filtration pool of MIOX activity. The activity pool from S-200 gel filtration was concentrated by ultrafiltration on an Amicon YM-10 membrane and filtered through a 0.2 mm syringe filter before HPLC. Samples containing approx. 3 mg of protein in 1 M $(NH_4)_2SO_4$ were chromatographed on a SigmaChrom phenyl-HIC HPLC column and eluted at 0.9 ml/min with standard buffer containing the indicated salt gradient (dotted line). The box denotes the range of eluate collected from several HPLC runs and combined as the 'HIC activity pool.' (**B**) SDS/PAGE analysis of eluate fractions from the HIC purification step. Right lane: MIOX preparation after HIC purification step was examined on an SDS/PAGE gel with Coomassie Blue staining for proteins. The amount of pig MIOX loaded was 4 μg. Left lane: molecular mass markers (molecular masses indicated in kDa at the left).

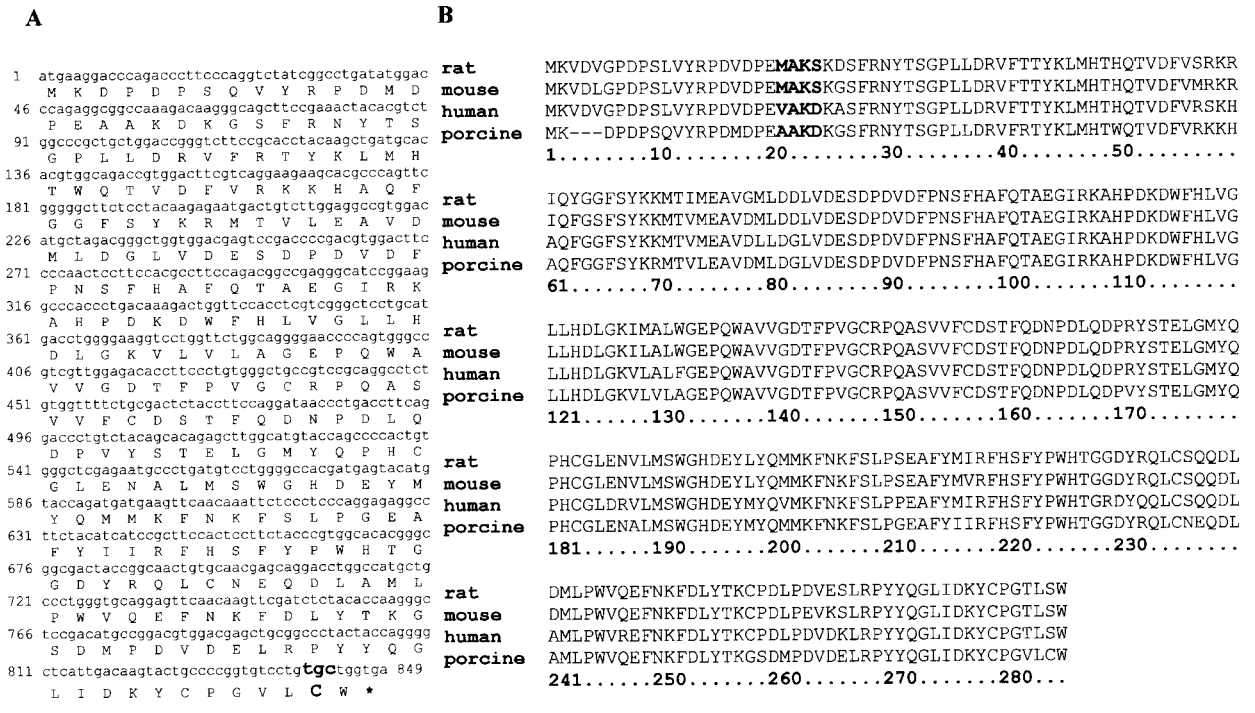

Figure 3 Open reading frame and alignment of deduced primary sequence of pig MIOX with hypothetical protein sequences

(**A**) The nucleotide sequence of the open reading frame of pig kidney MIOX and its deduced amino acid sequence are shown. A cysteine residue unique with regard to reported sequences in other species is indicated in bold. (**B**) Alignment of the amino acid sequences of pig MIOX and the sequences reported by Yang et al. [34]. The NADPH-binding motif found in the mouse sequence is indicated in bold. Accession numbers are as follows: rat, AF197128; mouse, AF197127; human, AF197129; pig, AF401311.

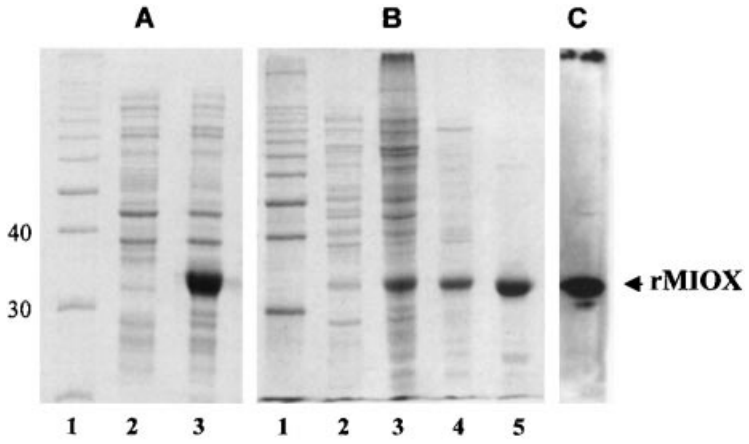

Figure 4 SDS/PAGE of rMIOX at different stages of purification

(**A**) SDS/PAGE of total cellular lysates of BL21(DE3) cells, prepared with 2% (w/v) SDS, expressing rMIOX after induction with 1 mM IPTG. Lane 1, 10 kDa marker (Gibco-BRL); lane 2, uninduced cells; lane 3, after 4 h of induction with IPTG. (**B**) SDS/PAGE of the expressed rMIOX purification. Lane 1, 10 kDa ladder; lane 2, crude cell lysate (supernatant of ground and sonicated cells); lane 3, 35–60%-satd $(NH_4)_2SO_4$ fraction; lane 4, DE-52 active pooled fractions; lane 5, S-200 gel-filtration pooled active fractions. The load per lane was 4 μg. (**C**) Western immunoblot analysis of the purified rMIOX with monoclonal antibodies prepared against native pig MIOX. The numbers at the left are molecular masses in kDa.

towards *myo*-inositol. The HIC-purified MIOX preparation was used for obtaining internal peptide sequences, which were then used to generate primer sequences for PCR cloning from the pig kidney cDNA library.

Cloning of MIOX cDNA

A cDNA was PCR amplified from the pig kidney library containing the open reading frame of 849 bp (Figure 3A), as well as 5′ and 3′ untranslated region sequences totalling approx. 1.1 kb. Northern blot analysis indicated that the transcript was approx. 1.6 kb in length. A BLAST search conducted with National Center for Biotechnology Information online software revealed that the sequence was unique, with the only matches to sequences of hypothetical cDNA submissions (accession numbers AF197127, AF197129, AF197128) by Yang et al. [34], and a partial match to *Pinus radiata* sequence (accession number AF049069). The degree of similarity was approx. 86–89% to the rat and mouse sequences and 96% to the human sequence (Figure 3B). One major difference between our sequence and those of hypothetical submissions by Yang et al. was found in the N-terminus of the protein sequence. Amino acids (VDL/V; single-letter amino acid codes) found in the rat, mouse and human hypothetical sequences after the N-terminal methionine were missing from the pig sequence. Furthermore, the NADPH-binding motif sequence (MAKS) found in mouse and rat was also missing from the pig MIOX sequence, especially the essential serine residue. Instead, the pig sequence contained AAKD, which is similar to the human sequence (VAKD). The hypothetical sequences had six cysteine residues conserved at positions 147, 156, 182, 234, 257 and 278. The pig sequence also had cysteine residues at all these positions except at 257 where it was glycine instead of cysteine. The sixth cysteine residue in pig sequence was present as the penultimate amino acid at the C-terminal end (Figure 3B). The hypothetical sequences from other species had a conserved serine at this position. There were a total of ten histidine residues in the pig sequence, nine of which were common to those reported for the hypothetical sequences in rat, mouse and human. The histidine residue present at the 49th position in rat, mouse and human was missing from the pig sequence, where it was tryptophan. Instead, the tenth histidine residue in pig was present at position 59. Interestingly, the human hypothetical sequence also had an additional histidine residue at this position, whereas the rat and mouse hypothetical sequences had arginine (Figure 3B).

Expression and purification of rMIOX

The pET17b/MIOX construct was transformed into BL21(DE3) cells and significant MIOX expression was observed after 4 h of induction with IPTG by SDS/PAGE analysis (Figure 4A, lane 3). Owing to interference in the orcinol assay at very low levels, detergents could not be used in the lysis and purification procedures for rMIOX. Instead, steps were performed in the standard buffer. As can be seen in the purification table (Table 1) and SDS/PAGE (Figure 4B, lane 5), the final rMIOX preparation was more than 95% pure, with a specific activity higher than that of the native enzyme. However, the yield of active MIOX in soluble fraction was relatively low, which seems to have been due to a large percentage of the rMIOX going into the insoluble inclusion bodies. Total cell-free extracts prepared in the presence of detergent showed that the amount of 33 kDa protein produced by BL21(DE3) cells induced with IPTG was indeed substantial (more than 10 mg/l; see Figure 4A, lane 3). Attempts were made to isolate the rMIOX from the purified inclusion bodies; however, the protein was inactive. Experiments designed to refold it were unsuccessful (results not shown). Supplementing the LB medium with 20 mM *myo*-inositol improved yields 2–3-fold in the soluble fraction. Media conditions for higher expression in the soluble fraction are being examined.

Characterization of rMIOX

The subunit molecular mass based on the translated amino acid sequence for the rMIOX cDNA was calculated to be 32.7 kDa. This was checked by SDS/PAGE (Figure 4B, lane 5) and electrospray MS. Results from MS indicated the molecular mass to be 32.663 kDa. In addition, gel-permeation chromatography on Sephacryl 200 was used to calculate the molecular mass of the rMIOX, which was found to co-elute with bovine erythrocyte

Table 1 Summary of the purification of recombinant MIOX from *E. coli*

The enzyme was purified from 2 litres of LB medium induced with 1 mM IPTG for 4 h as described in the Experimental section.

Step	Total protein (mg)	Total activity (nmol/min)	Specific activity (nmol/min per mg)	Yield (%)
Crude lysate	57.0	2268	40	100
35–60%-satd $(NH_4)_2SO_4$ fraction	18.0	2449	134	108
DE-52 column chromatography	5.0	1735	359	76
Sephacryl 200 column chromatography	0.8	1295	1546	57

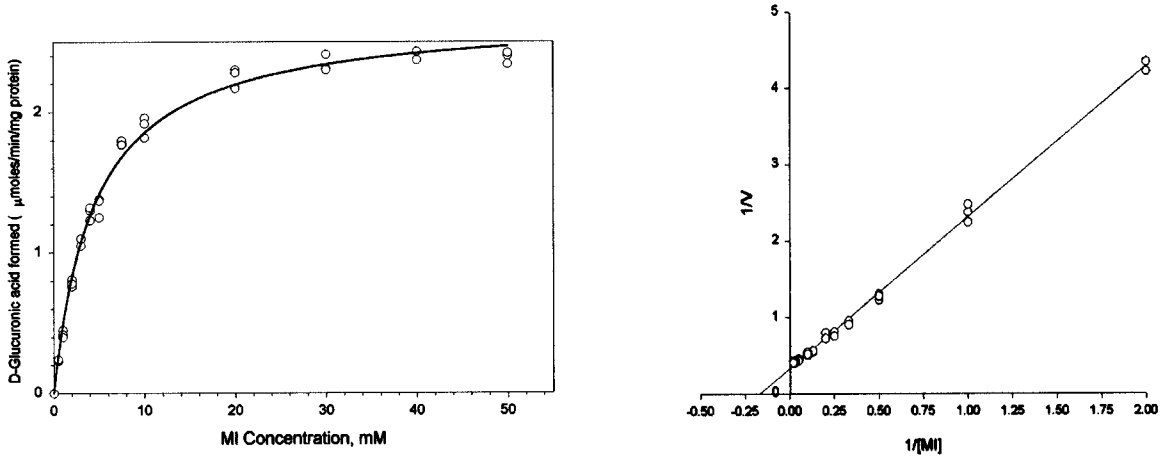

Figure 5 Substrate kinetics of the oxidation of *myo*-inositol by rMIOX

Left panel: the concentration of *myo*-inositol (MI) was varied from 0.5 to 50 mM and the product, D-glucuronate, was assayed as described in the Experimental section. Right panel: Lineweaver–Burk plot.

superoxide dismutase (molecular mass 32.5 kDa). Western immunoblot analysis with the monoclonal antibodies prepared against the native pig MIOX confirmed the identity of expressed rMIOX (Figure 4C). The subunit molecular mass was confirmed by sedimentation equilibrium analysis. In addition, this analysis revealed that rMIOX did not dimerize on the addition of *myo*-inositol or *myo*-inositol plus Fe^{2+}/cysteine to the enzyme. This is in contrast with the substrate-dependent oligomerization reported previously [35] for the rat kidney native MIOX.

An isoelectric focusing gel was run with two sets of standards (Sigma). The pI of MIOX was found to be 4.5 (results not shown), in agreement with the earlier studies on native MIOX from our group [10,11]. The enzymic activity, as determined by orcinol assay, was found to be heat labile and dependent on *myo*-inositol. As described previously by our group, the activity was also dependent on activation by Fe^{2+} and cysteine. This was accomplished by incubating the recombinant protein with 1 mM ferrous ammonium sulphate and 2 mM L-cysteine for 7 min before the addition of substrate. Other thiol compounds such as GSH, 2-mercaptoethanol and lipoic acid were tested and none were found to replace cysteine in the reaction, nor were they inhibitory. Kinetic parameters of rMIOX were in agreement with those reported previously [10,11]. The K_m for *myo*-inositol was 5.9 mM and the k_{cat} was 11 min^{-1} (Figure 5). The affinity for D-*chiro*-inositol was less than that of *myo*-inositol; the K_m and k_{cat} for D-*chiro*-inositol were estimated to be 33.5 mM and 2.3 min^{-1} respectively (results not shown). However, the kinetic parameters for the latter substrate could not be calculated accurately because the product of the reaction and its orcinol conjugate have not been characterized.

Yang et al. [34] reported NADPH binding for the mouse hypothetical protein, which they named as aldehyde reductase 6. Since our protein had 86% similarity to the hypothetical mouse protein, we examined the binding of rMIOX to a Reactive Blue Agarose column. No binding was detected because the flow-through fractions contained more than 95% of the MIOX protein.

DISCUSSION

MIOX is of considerable interest physiologically because it catalyses the first committed step in the only pathway of *myo*-inositol catabolism and it occurs predominantly in the kidney. Clearly this reaction is an important determinant of the inositol levels *in vivo*. One metabolic disease in which the enzyme might be especially significant is diabetes mellitus. Diabetics excrete excessive amounts of inositol in their urine and it seems that in addition to glucose interference with inositol transport, decreased activity of MIOX might also be involved [36]. Among other effects, the alterations of tissue levels of inositol in diabetics are believed to contribute to diabetic neuropathy. More recently, even greater attention has been focused on inositol metabolism because it has become clear that various inositol derivatives, especially the trisphosphates, act as second messengers in various signal transduction pathways in mammalian cells. In addition, MIOX is of considerable interest owing to its unusual mono-

oxygenase mechanism in which the ring of *myo*-inositol is cleaved with the incorporation of one atom of oxygen [12]. There are very few enzymes that catalyse an oxidative glycol cleavage reaction in this way.

We have now isolated and sequenced a cDNA clone encoding MIOX from pig kidney and expressed the rMIOX protein in bacteria. The bacterial expression system produces reasonable amounts of soluble and active MIOX and the expression is further enhanced 3-fold on supplementation of the medium with *myo*-inositol. However, most MIOX is found in inclusion bodies and attempts to refold it have not been successful. The enzyme is a 32.7 kDa protein that shows no significant sequence similarity to any known proteins. However, pig MIOX cDNA sequence has 86–89 % similarity to the rat and mouse clones of Yang et al. [34], which were reported as possible members of the aldo–keto reductase (AKR) family of enzymes. Whereas the mouse clone product examined by Yang et al. bound strongly to NADPH, no such interaction was observed with the pig rMIOX in terms of binding to Blue Agarose. This seems likely to be due to a mutation of an essential serine residue in the NADPH-binding domain. The human clone also lacks the serine and has a similar sequence to that of the pig clone in this region (Figure 3B). Furthermore, as in other Fe–sulphur-cluster-containing proteins, the presence of conserved histidine and cysteine residues in MIOX might indicate a potential role for these residues in enzyme function.

As mentioned above, a rat clone for a hypothetical protein has been sequenced, the sequence of which is almost identical with the mouse sequence and very similar to that of pig MIOX [34]. Although the authors reported it as a protein of the aldehyde reductase (ALR) family, it is conceivable that it could be MIOX. However, if this hypothetical protein in rat is indeed MIOX, this needs to be reconciled with the work of Koller and colleagues [35,37,38], who have extensively characterized the rat enzyme and shown MIOX to be an oligomer of 17 kDa subunits. Thus there is a considerable discrepancy between the subunit molecular mass of the native enzyme from rat kidney (17 kDa) and the predicted value from the reported hypothetical rat transcript, which is approximately double the size [34]. Our results with pig rMIOX prove convincingly that the pig protein has a molecular mass of 32.7 kDa and, in contrast with Koller's observations [35,37,38], does not undergo oligomerization in the presence of *myo*-inositol.

Previously we had reported that the native MIOX enzyme is probably found in a complex with the enzyme responsible for the second step of *myo*-inositol catabolism, namely glucuronate reductase [10], which is also known as aldehyde reductase or ALR1 (EC 1.1.1.2) [39]. It was subsequently demonstrated that glucuronate reductase prefers the acyclic form of glucuronate [40]. When glucuronate was replaced with stoichiometric equivalents of MIOX and *myo*-inositol in the glucuronate reductase assays, a greater consumption of NADPH was observed than an equivalent amount of free glucuronate, which is predominantly in the cyclic form. It is presumed that MIOX can transfer the acyclic glucuronate directly to the reductase in the complex [10]. Currently we are examining the interactions of MIOX with expressed pig kidney ALR1 *in vitro* with a yeast two-hybrid system.

Because *myo*-inositol homoeostasis is altered in diabetes mellitus, we are increasingly interested in the role of MIOX in this disease. Renal clearance of *myo*-inositol in diabetic patients and diabetic rats has been shown to increase up to severalfold relative to control subjects. At the same time, kidney MIOX activity levels have been observed to decrease an average of 4-fold relative to controls [36]. In contrast, recent data from Yang et al. [34] show that the message levels of the mouse hypothetical protein are increased in diabetes. Although altered MIOX activity has not been localized within the kidney, a report has shown significant differences in MIOX distribution between the cortex and medulla in perinatal rabbit kidney [27]. However, there is a large body of literature to indicate that tissue levels of *myo*-inositol are decreased significantly in response to hyperglycaemia caused by diabetes, along with an accumulation of sorbitol. This decrease in inositol levels is thought to be a major factor in diabetic complications [17]. Because of this conflicting evidence, the exact role of MIOX in diabetes remains unclear.

We thank Dr Robert Simpson for performing sedimentation equilibrium experiments in his laboratory. We also thank Dr Gordon A. Hamilton for allowing us to take over this project on his retirement as well as for his continued valuable discussions. This work was funded in part by National Institutes of Health grants HL06347-02 and DK49122-05.

REFERENCES

1 Holub, B. J. (1986) Metabolism and function of *myo*-inositol and inositol phospholipids. Annu. Rev. Nutr. **6**, 563–597
2 Majerus, P. W. (1992) Inositol phosphate biochemistry. Annu. Rev. Biochem. **61**, 225–250
3 Loewus, F. A. and Loewus, M. W. (1983) *Myo*-inositol: its biosynthesis and metabolism. Annu. Rev. Plant Physiol. **34**, 137–161
4 Howard, C. F. and Anderson, L. (1967) Metabolism of *myo*-inositol in animals. II. Complete catabolism of *myo*-inositol-^{14}C by rat kidney slices. Arch. Biochem. Biophys. **118**, 332–339
5 Charalampous, F. C. and Lyras, C. (1957) Biochemical studies on inositol. IV. Conversion of inositol to glucuronic acid by rat kidney extracts. J. Biol. Chem. **228**, 1–13
6 Hankes, L. V., Politzer, W. M., Touster, O. and Anderson, L. (1969) *Myo*-inositol catabolism in human pentosurics: the predominant role of the glucuronate-xylulose-pentose phosphate pathway. Ann. N.Y. Acad. Sci. **165**, 564–576
7 Charalampous, F. C. (1959) Biochemical studies on inositol. V. Purification and properties of the enzyme that cleaves inositol to D-glucuronic acid. J. Biol. Chem. **234**, 220–227
8 Charalampous, F. C. (1960) Biochemical studies on inositol. IV. Conversion of inositol to glucuronic acid by rat kidney extract. J. Biol. Chem. **5**, 1286–1291
9 Koller, E., Koller, F. and Hoffmann-Ostenhof, O. (1976) *Myo*-inositol oxygenase from oat seedlings. Mol. Cell Biochem. **10**, 33–39
10 Reddy, C. C., Swan, J. S. and Hamilton, G. A. (1981) *myo*-Inositol oxygenase from hog kidney. I. Purification and characterization of the oxygenase and of an enzyme complex containing the oxygenase and D-glucuronate reductase. J. Biol. Chem. **256**, 8510–8518
11 Reddy, C. C., Pierzchala, P. A. and Hamilton, G. A. (1981) *myo*-Inositol oxygenase from hog kidney. II. Catalytic properties of the homogeneous enzyme. J. Biol. Chem. **256**, 8519–8524
12 Moskala, R., Reddy, C. C., Minard, R. D. and Hamilton, G. A. (1981) An oxygen-18 tracer investigation of the mechanism of *myo*-inositol oxygenase. Biochem. Biophys. Res. Commun. **99**, 107–113
13 Hamilton, G. A., Reddy, C. C., Swan, J. S., Moskala, R., Mulliez, E. and Naber, N. I. (1982) Mechanistic aspects of oxygenases in general and *myo*-inositol oxygenase in particular. In Oxygenases and Oxygen Metabolism (Nozaki, M., Yamamoto, S. and Ishimura, Y., eds.), pp. 111–123, Academic Press, New York
14 Payrastre, B., Missy, K., Giuriato, S., Bodin, S., Plantavid, M. and Gratacap, M. (2001) Phosphoinositides: key players in cell signalling, in time and space. Cell Signal. **13**, 377–387
15 Goraya, T. Y., Wilkins, P., Douglas, J. G., Zhou, J. and Berti-Mattera, L. N. (1995) Signal transduction alterations in peripheral nerves from streptozotocin-induced diabetic rats. J. Neurosci. Res. **41**, 518–525
16 Palmano, K. P., Whiting, P. H. and Hawthorne, J. N. (1977) Free and lipid *myo*-inositol in tissues from rats with acute and less severe streptozotocin-induced diabetes. Biochem. J. **167**, 229–235
17 Winegrad, A. I. (1987) Banting Lecture 1986. Does a common mechanism induce the diverse complications of diabetes? Diabetes **36**, 396–406
18 Larner, J., Allan, G., Kessler, C., Reamer, P., Gunn, R. and Huang, L. C. (1998) Phosphoinositol glycan derived mediators and insulin resistance. Prospects for diagnosis and therapy. J. Basic Clin. Physiol. Pharmacol. **9**, 127–137
19 Cohen, A. M., Wald, H., Popovtzer, M. and Rosenmann, E. (1995) Effect of *myo*-inositol supplementation on the development of renal pathological changes in the Cohen diabetic (type 2) rat. Diabetologia **38**, 899–905

20 Cohen, M. P. (1986) Aldose reductase, glomerular metabolism, and diabetic nephropathy. Metabolism **35**, 55–59
21 Narayanan, S. (1993) Aldose reductase and its inhibition in the control of diabetic complications. Ann. Clin. Lab. Sci. **23**, 148–158
22 Henry, D. N., Del Monte, M., Greene, D. A. and Killen, P. D. (1993) Altered aldose reductase gene regulation in cultured human retinal pigment epithelial cells. J. Clin. Invest. **92**, 617–623
23 Benfield, P. (1986) Aldose reductase inhibitors and late complications of diabetes. Drugs. **32**(suppl. 2), 43–55
24 Dyck, P. J., Minnerath, S. R. and O'Brien, P. C. (1989) Nerve glucose, sorbitol, fructose, and *myo*-inositol at various time after feeding in streptozotocin-induced diabetes in rats. Mayo Clin. Proc. **64**, 905–910
25 Goode, D., Lewis, M. E. and Crabbe, M. J. (1996) Accumulation of xylitol in the mammalian lens is related to glucuronate metabolism. FEBS Lett. **395**, 174–178
26 Lin, L. R., Reddy, V. N., Giblin, F. J., Kador, P. F. and Kinoshita, J. H. (1991) Polyol accumulation in cultured human lens epithelial cells. Exp. Eye Res. **52**, 93–100
27 Bry, K. and Hallman, M. (1991) Perinatal development of inositol synthesis and catabolism in rabbit kidney. Biol. Neonate **60**, 249–257
28 Pfeifer, M. A. and Schumer, M. P. (1995) Clinical trials of diabetic neuropathy: past, present, and future. Diabetes **44**, 1355–1361
29 Raccah, D., Coste, T., Cameron, N. E., Dufayet, D., Vague, P. and Hohman, T. C. (1998) Effect of the aldose reductase inhibitor tolrestat on nerve conduction velocity, Na/K ATPase activity, and polyols in red blood cells, sciatic nerve, kidney cortex, and kidney medulla of diabetic rats. J. Diabetes Complic. **12**, 154–162
30 Fonteles, M. C., Huang, L. C. and Larner, J. (1996) Infusion of pH 2.0 D-*chiro*-inositol glycan insulin putative mediator normalizes plasma glucose in streptozotocin diabetic rats at a dose equivalent to insulin without inducing hypoglycaemia. Diabetologia **39**, 731–734
31 Fonteles, M. C., Almeida, M. Q. and Larner, J. (2000) Antihyperglycemic effects of 3-O-methyl-D-*chiro*-inositol and D-*chiro*-inositol associated with manganese in streptozotocin diabetic rats. Horm. Metab. Res. **32**, 129–132
32 Ostlund, Jr, R. E., McGill, J. B., Herskowitz, I., Kipnis, D. M., Santiago, J. V. and Sherman, W. R. (1993) D-*chiro*-Inositol metabolism in diabetes mellitus. Proc. Natl. Acad. Sci. U.S.A. **90**, 9988–9992
33 Ostlund, Jr, R. E., Seemayer, R., Gupta, S., Kimmel, R., Ostlund, E. L. and Sherman, W. R. (1996) A stereospecific *myo*-inositol/D-*chiro*-inositol transporter in HepG2 liver cells. Identification with D-*chiro*-[3-^{3}H]inositol. J. Biol. Chem. **271**, 10073–10078
34 Yang, Q., Dixit, B., Wada, J., Tian, Y., Wallner, E. I., Srivastva, S. K. and Kanwar, Y. S. (2000) Identification of a renal-specific oxido-reductase in newborn diabetic mice. Proc. Natl. Acad. Sci. U.S.A. **97**, 9896–9901
35 Koller, F. and Koller, E. (1990) *myo*-inositol oxygenase from rat kidneys. Substrate-dependent oligomerization. Eur. J. Biochem. **193**, 421–427
36 Whiting, P. H., Palmano, K. P. and Hawthorne, J. N. (1979) Enzymes of *myo*-inositol and inositol lipid metabolism in rats with streptozotocin-induced diabetes. Biochem. J. **179**, 549–553
37 Koller, F. and Hoffmann-Ostenhof, O. (1979) *myo*-Inositol oxygenase from rat kidneys. I: Purification by affinity chromatography; physical and catalytic properties. Hoppe-Seylers Z. Physiol. Chem. **360**, 507–513
38 Koller, F. and Koller, E. (1984) Affinity chromatography of *myo*-inositol oxygenase from rat kidney by means of an insoluble D-galacto-hexodialdose derivative. J. Chromatogr. **283**, 191–197
39 De Jongh, K. S., Schofield, P. J. and Edwards, M. R. (1987) Kinetic mechanism of sheep liver NADPH-dependent aldehyde reductase. Biochem. J. **242**, 143–150
40 Naber, N. I. and Hamilton, G. A. (1987) Concerning the mechanism for transfer of D-glucuronate from *myo*-inositol oxygenase to D-glucuronate reductase. Biochim. Biophys. Acta **911**, 365–368

Received 8 August 2001/5 September 2001; accepted 24 September 2001